Eur Biophys J (2000) 28: 648–662

ARTICLE

Nicolas Sajot · Monique Genest

Structure prediction of the dimeric neu/ErbB-2 transmembrane domain from multi-nanosecond molecular dynamics simulations

Received: 12 March 1999 / Revised version: 23 August 1999 / Accepted: 23 August 1999

Abstract Dimerization of the neu/ErbB-2 receptor tyrosine kinase is a necessary but not a sufficient step for signaling. Despite the efforts expended to identify the molecular interactions responsible for receptor-receptor contacts and particularly those involving the transmembrane domain, structural details are still unknown. In this work, molecular dynamics simulations of the helical transmembrane domain (TM) of neu and ErbB-2 receptors are used to predict their dimer structure both in the wild and oncogenic forms. A global conformational search method, applied to define the best orientations of parallel helices, showed an energetically favorable configuration with the specific mutation site within the interface, common for both the nontransforming and the transforming neu/ErbB-2 TM dimers. Starting from this configuration, a total of 10 simulations, about 1.4 ns each, performed in vacuum, without any constraints, show that the two helices preferentially wrap in left-handed interactions with a packing angle at about 20°. The resulting structures are nonsymmetric and the hydrogen bond network analysis shows that helices experience π local distortions that facilitate interhelix hydrogen bond interactions and may result in a change in the helix packing, leading to a symmetric interface. For the mutated sequences, we show that the Glu side chain interacts directly with its cognate or with carbonyl groups of the facing backbone. We show that the connectivity between interfacial residues conforms to the knobs-into-holes packing mode of transmembrane helices. The dimeric interface described in our models is discussed with respect to mutagenesis studies.

Key words neu/ErbB-2 receptors · Molecular dynamics simulations · Transmembrane helix · Dimer structure · Left-handed coiled coil

N. Sajot · M. Genest (✉)
Centre de Biophysique Moléculaire, UPR 4301, CNRS, affiliated to the University of Orléans, rue Charles Sadron, F-45071 Orléans Cédex 02, France
e-mail: m.genest@cnrs-orleans.fr

Introduction

Ligand-induced dimerization of receptor protein tyrosine kinase is a fundamental step to stimulate the intracellular tyrosine kinase activity (Ullrich and Schlessinger 1990). Receptor-receptor interactions in which the transmembrane domain or the cytoplasmic domain or both are involved were first supported by studies on the epidermal growth factor receptor (EGFR) (Yarden and Schlessinger 1987). Similar inter-receptor contacts within the membrane-spanning domain of the rat neu and the human ErbB-2 receptors, two members of the EGFR family, have been identified (Coussens et al. 1985; Bargmann et al. 1986; Yamamoto et al. 1986). The particularity of the transmembrane domain (TM) of these receptors resides in the single point mutation Val → Glu that leads to a considerable increase of receptor dimerization and tyrosine kinase activity (Bargmann and Weinberg 1988; Stern et al. 1988; Weiner et al. 1989a, b). This mutation at position 664 in neu has not been identified in human cancers (Lemoine et al. 1990), but produces the same transforming effect when it is introduced experimentally at the homologous position 659 in ErbB-2 (Segatto et al. 1988). The hypothesis of a key role played by the single transmembrane domain in the receptor dimerization process is supported by the identification of other intramembrane mutations responsible for transformation as for EGFR (Miloso et al. 1995), the insulin receptor (Longo et al. 1992), and the fibroblast growth factor receptor 3 that leads to human dwarfism (Rousseau et al. 1994; Shiang et al. 1994; Webster and Donoghue 1996). Because of the potential therapeutic use of transmembrane peptides to interfere with signaling (Lofts et al. 1993; Hynes and Stern 1994), many studies have been undertaken to elucidate the mechanisms of dimerization by this mutation. Activating mutation was first suggested as acting to stabilize the transmembrane helix structure, favoring inter-receptor packing (Brandt-Rauf et al. 1990), but alternatively it was thought that the Glu mutation might

act directly in contacting its cognate or other amino acids (Sternberg and Gullick 1989). The first hypothesis of intramolecular effects can be paralleled by the difference in structure and flexibility between the wild and the oncogenic ErbB-2 TM detected from molecular dynamics (MD) simulations (Garnier et al. 1994). However, further MD studies on other mutated sequences have proved a minor role for the mutating residue in helix flexibility (Duneau et al. 1997). The second hypothesis based on intermolecular contacts, that seems to prevail but without totally excluding intramolecular conformational changes in helices, is supported by experiments which evidence Glu-Glu side chain interactions between neu TM helices embedded in lipid bilayers (Smith et al. 1996). Similar interactions have been identified from MD simulations on ErbB-2 TM helix association (Garnier et al. 1997).

Occurrence of intramembrane Glu residues in neu/ErbB-2 or in other activated receptors suggested that polar residues capable of hydrogen bonding in appropriate positions are sufficient to induce dimerization and activation (Longo et al. 1992; Jenkins et al. 1995; Miloso et al. 1995). Studies have shown that activation of the neu mutant can be achieved by simple heptad sequences of Val residues including a central Glu residue (Chen et al. 1997) an that it is sufficient to replace Val by Ala in the last position of the heptad motif to modulate the activation. This point was also addressed by evaluating the power of dimerization and transformation of a panel of neu mutants (Cao et al. 1992; Burke et al. 1997). These authors evidence the importance of the VEG tripeptide domain for transforming activity, but curiously this motif does not significantly enhance dimerization when it is introduced at alternative positions in the sequence. Additional sequence context, packing, or/and positional constraints are supposed to allow the triplet to function properly in enhancing dimerization.

The whole set of studies on neu/ErbB-2 let emerge important sites for TM dimerization (Sternberg and Gullick 1990; Burke et al. 1997) and the recent mutagenesis study by Burke and Stern (1998), which identifies a dimer interface, is a useful approach to give insight into specificity. Nevertheless, the ability of a Glu residue to activate a particular TM domain and the dependence of its position upon sequence-specific details is not yet understood.

To progress in neu/ErbB-2 signal transduction it seems necessary to investigate molecular interactions that drive their TM association. These are still lacking owing to the experimental difficulties of studying membrane proteins.

An alternative method to better understand the molecular details of activating mutations in neu/ErbB-2 is to use predictive methods based on molecular modeling and MD simulations. We have successfully used these techniques to propose one dimer structure for ErbB-2 TM (Garnier et al. 1997), close to a model suggested from experimental data (Smith et al. 1996). To further out knowledge of TM interactions we extend our prediction on ErbB-2 and neu, which exhibits large sequence homology. The aim of this study is to improve the previously determined model that predicted left-handed interactions between the two helices. In this work, we examine one structure produced from a global searching method, with the two uncoiled helices exhibiting the mutation site at the helix-helix interface and found energetically favorable for both the transforming and the nontransforming types for neu and ErbB-2. A series of simulations, about 1.4 ns each, show that the two helices cross in left-handed interactions at about 20° practically for all the cases. A detailed analysis of the interacting helices is presented for the different models obtained in relation to the internal structure of the helices and hydrogen bonded interactions. The dimeric interface defined from our simulations is asymmetric and shows common features with the dimeric interface proposed on the basis of mutagenesis studies.

Methods

Programs and calculation parameters

The structure of the TM is the canonical α helix built with the SYBYL package (Tripos Associates). The initial side chain rotamers are those provided by the attached library giving the preferential rotamers of residues in the secondary helix structure (Dunbrack and Karplus 1993). All calculations employ the GROMOS force field (van Gunsteren 1987) using the "in vacuum" parameters and considering a united atom representation for the aliphatic hydrogen atoms and explicit polar hydrogen atoms. A value of 1 for the dielectric constant is used to implicitly model the low dielectric environment within a membrane bilayer. In all calculations involving energy minimization and MD simulations, no distance constraints are applied on the α hydrogen bond network of the backbone nor anywhere else. The nonbonded interactions, including van der Waals and electrostatic one, are evaluated without distance truncation.

neu/ErbB-2 dimer models

The peptides have the sequence of the whole TM that extends from Leu651 to Ile675 for ErbB-2 and from Val656 to Ile680 for neu (Fig. 1). Their extremities are capped by the acetyl and methylamine blocking groups at the amino and carbonyl termini, respectively. The Pro residue at the N-terminus of the transmembrane sequence and the highly polar residues Arg, Lys, and Gln at the C-terminus, which act as a stop signal at the membrane interfaces, are not included in our model. The 25 residues, numbered from 1 to 25, constitute the hydrophobic part of the TM and the mutation site is at position 9. The Glu664/659 mutated transmembrane sequences of neu/ErbB-2 are obtained by replacing Val9 by Glu9. In

neu	656	657	658	659	660	661	662	663	664	665	666	667	668	669	670	671	672	673	674	675	676	677	678	679	680
	Val	Thr	Phe	Ile	Ile	Ala	Thr	Val	Val	Gly	Val	Leu	Leu	Phe	Leu	Ile	Leu	Val	Val	Val	Val	Gly	Ile	Leu	Ile
	1	2	3	4	5	6	7	8	9	10	11	12	13	14	15	16	17	18	19	20	21	22	23	24	25
ErbB-2	Leu	Thr	Ser	Ile	Ile	Ser	Ala	Val	Val	Gly	Ile	Leu	Leu	Val	Val	Val	Leu	Gly	Val	Val	Phe	Gly	Ile	Leu	Ile
	651	652	653	654	655	656	657	658	659	660	661	662	663	664	665	666	667	668	669	670	671	672	673	674	675

Fig. 1 Sequence of the neu/ErbB-2 transmembrane domains used in molecular dynamics simulations. The residues conserved between the two sequences are *shaded*

all calculations, the Glu side chain is considered in the protonated state, in accord with experimental studies on the complete neu TM (Smith et al. 1996). This same assumption was also made in our previous studies (Garnier et al. 1994; Duneau et al. 1996, 1997).

Global search for dimer configurations

The search for stable low-energy conformations of the dimer structures was carried out in two steps and the strategy used in a previous study (Garnier et al. 1997) is here resumed.

The initial dimer configuration consists of two parallel identical α helices, named H1 and H2, separated by a distance *Dh* between the helical axes. H2 is obtained by translating a copy of H1 along the *X* axis defined by the vector joining the first Cα atom and its projection onto the H1 helical axis (taken as the *Z* axis).

The first step of the global search is to determine the best value for helix-helix separation giving rise to attractive intermolecular energy. For that, each helix, assumed as a rigid body, is rotated by 360° by steps of 18° about its helical axis. The set of 400 configurations obtained was examined by calculating the intermolecular energy evaluated as the summation of the nonbonded van der Waals and electrostatic terms. This is repeated for different values of *Dh*. For the wild and the mutated neu sequences, the best distance of separation is found at 1.11 nm; for the wild and the mutated ErbB-2 sequences it is found at 1.07 nm.

The second step is to determine the configurations of lowest energy for the determined distance *Dh*. The 400 configurations, characterized by the rotation angles $\theta 1$ and $\theta 2$ about the helical axes of H1 and H2 respectively, are then energy minimized. The zero value for $\theta 1$ and $\theta 2$ corresponds to the Cα atom of the first residue lying on the *X* axis. All the terms of the GROMOS force field are used in this stage, and the total potential energy of the dimer is calculated as the sum of the potential energy of each helix (intramolecular energy) and the potential energy between the two helices (intermolecular energy). Since no distance constraints are used, the two helices are totally free to optimize their interactions, particularly through χ dihedral angle rotations of the side chains, helix-helix separation, and backbone distortions.

This protocol, previously used to identify the most probable low-energy configurations of the ErbB-2 TM dimers, is repeated for the wild and the mutated neu TM.

neu/ErbB-2 model refinement

MD techniques were used to optimize helix-helix interactions with the aim of guiding the two straight parallel helices towards the best helix packing. No constraints were applied to the system, permitting helix structure modulation, helix bending, variation in helix separation, and helix shift. The MD protocol begins by a heating period during which the system was gradually thermalized from 0 to 300 K by increments of 50 K for 2 ps. New atomic random velocities were reassigned from a Maxwell distribution at each temperature step. Constant temperature was maintained by a strong coupling to a heat bath (relaxation time 0.01 ps) all along the heating period. Equilibration was continued for several hundreds of ps with a low coupling (relaxation time 0.1 ps) and followed by a production period for about 1 ns. The SHAKE algorithm (Berendsen et al. 1984) was not applied and a short time step of 0.0005 ps was used for the integration of motion equations. Atomic and energy trajectories were stored every 0.05 ps.

To ensure a good convergence, each simulation was reproduced several times starting from different initial atomic velocities. For ErbB-2 TM, three simulations were carried on the wild type referred to as E1, E2, E3, and two simulations were carried on the oncogenic type referred to as E1* and E2*. For neu TM, two simulations were carried on the wild type referred to as N1, N2 and three on the mutated type referred to as N1*, N2*, N3*. The timescale of each simulation ranges from 1320 to 1380 ps. The last hundreds of ps of the simulations were considered as representative of the behavior of neu/ErbB-2 TM helices in homodimeric association.

Simulation analysis

Energy

Time series of the van der Waals and electrostatic energies were plotted to check the stability of the simulations and to detect conformational transitions. The mean structures are obtained by averaging the last hundreds of ps (120–270 ps), depending upon the stability of the simulations. For structure N2*, the analysis period is equal to 480 ps.

Hydrogen bonds

Dimer structures are characterized by the backbone hydrogen bond (HB) network of the two helices, which probes the helicity of each monomer and intra- and inter-helix HBs. Their residence time was calculated for the 10

simulations. It is expressed as the percentage value of HB existence during a defined period considering the following criteria. One HB exists when both the distance between the donor (D) and the acceptor (A) is less than 0.35 nm and the DHA angle is between 130° and 180°. The time series drawn to follow the dynamics of HB formation or HB rupture are smoothed over a 25 ps period.

Packing angle and helix separation

The crossing angle (Ω) measures the angle between the two helix axes. The helical axis is defined by the principal axis that corresponds to the lowest eigenvalue of the inertia tensor (longer axis) considering the coordinates of the helix backbone atoms (N, H, Cα, C, O) with all the atomic masses equal to unity. According to the definition used by Chothia et al. (1981), a negative angle of Ω characterizes a right-handed helix packing and a positive angle characterizes a left-handed helix packing.

Helix-helix separation is the distance computed between the geometric centers of a corresponding set of seven consecutive Cα atoms for both helices (Nilges and Brünger 1991; Garnier et al. 1997).

Inter-helix nearest-neighbor residues

The nearest-neighbor analysis is performed by using a home made program. The algorithm regards every residue of one helix having an atom in contact with an atom of a residue of the facing helix. Two atoms are considered in contact when their distance is within 0.06 nm of the sum of their van der Waals radii (aliphatic C 1.87 Å; C (CO, COOH) 1.76 Å; N 1.65 Å; O 1.40 Å; H 1.20 Å). This definition of contacting atoms used by Bowie (1997a, b) is equivalent to the rule that imposes a cutoff atomic distance of 0.45 nm (Langosch and Heringa 1998). Two residues are considered as contacting neighbors when at least three atoms of a residue are in contact with three atoms of a facing residue. This rule allows us to identify most of the neighboring residues. Additional contacts are identified from a graphical view of all the dimer structures. This leads to define distance criteria for "soft contacts" as follows: a "soft contact" exists when three atoms of one residue are within a distance of 0.65 nm with three atoms of a facing residue, one atomic pair, at least, having a distance greater than 0.45 nm. Such a strategy allows us to define almost all the neighboring residues that compose the helix-helix interface.

Results

Starting configuration

The potential energy surfaces obtained from the grid search method applied to neu/ErbB-2 TM for the wild and oncogenic types are given in Fig. 2. They show several low-energy configurations among which one, noted A, is common for the four dimer types and is located at rotation angles $\theta 1$ and $\theta 2$ equal to 90° and −162°, respectively. This state is the state of lowest energy for the wild type of neu and ErbB-2 with the values −1812 kJ/mol and −1850 kJ/mol, respectively. State A is a secondary minimum for the oncogenic type with an energy value of −2030 kJ/mol for neu and −2085 kJ/mol for the ErbB-2. The lowest state for the neu oncogenic type is found at $\theta 1$, $\theta 2$ = 270°, −90° (−2040 kJ/mol), and at $\theta 1$, $\theta 2$ = 126°, −144° (−2100 kJ/mol) for ErbB-2. This last state has been studied in a previous work (Garnier et al. 1997). In the present study we focus on state A, common for all cases.

Resulting coiled-coil structures

Crossing angle

The time series of the crossing angle calculated for the 10 simulations are shown in Fig. 3 and the angle values calculated for the energy minimized time-averaged structures are given in Table 1. The five simulations carried on neu TM dimers converge to a left-handed coiled-coil structure with a crossing angle ranging from 13° to 31°. The largest packing angle is obtained for the two simulations performed on the wild sequences, where the two helices wind round each other at 24° and 31°. For ErbB-2 TM dimers the final structures are more diversified, particularly for the wild type for which helices wrap round each other in a left or in a right sense or stand in a nearly parallel arrangement. When Glu replaces Val, left-handed coiled-coil interactions prevail with a packing angle of about 15–19°.

The time series reveal different pathways to reach the equilibrated structure. The left-handed structure initiates very early in the simulation, often during the heating period, and is maintained all along the simulation (E1, E1*, E2*, N2, N2*, N3*). In other cases, helices stand nearly parallel or are slightly right-handed wound (N1, N1*) before wrapping in the left sense. Two simulations do not follow this pathway of coiled coil formation. Simulation E2 shows that the two helices wound in the left sense at the beginning of the simulation rapidly wound in the right sense before adopting the parallel arrangement. Simulation E3 shows a transition between a left- and right-handed packing at about 1000 ps.

Helix-helix separation

The distances of closest approach calculated for the minimized averaged structures are given in Table 1. Helix-helix separation ranges between 0.945 and 1.030 nm for ErbB-2 and between 0.927 and 1.073 nm for neu, showing a significant decrease of the initial distance of separation up to 0.173 nm for neu. The

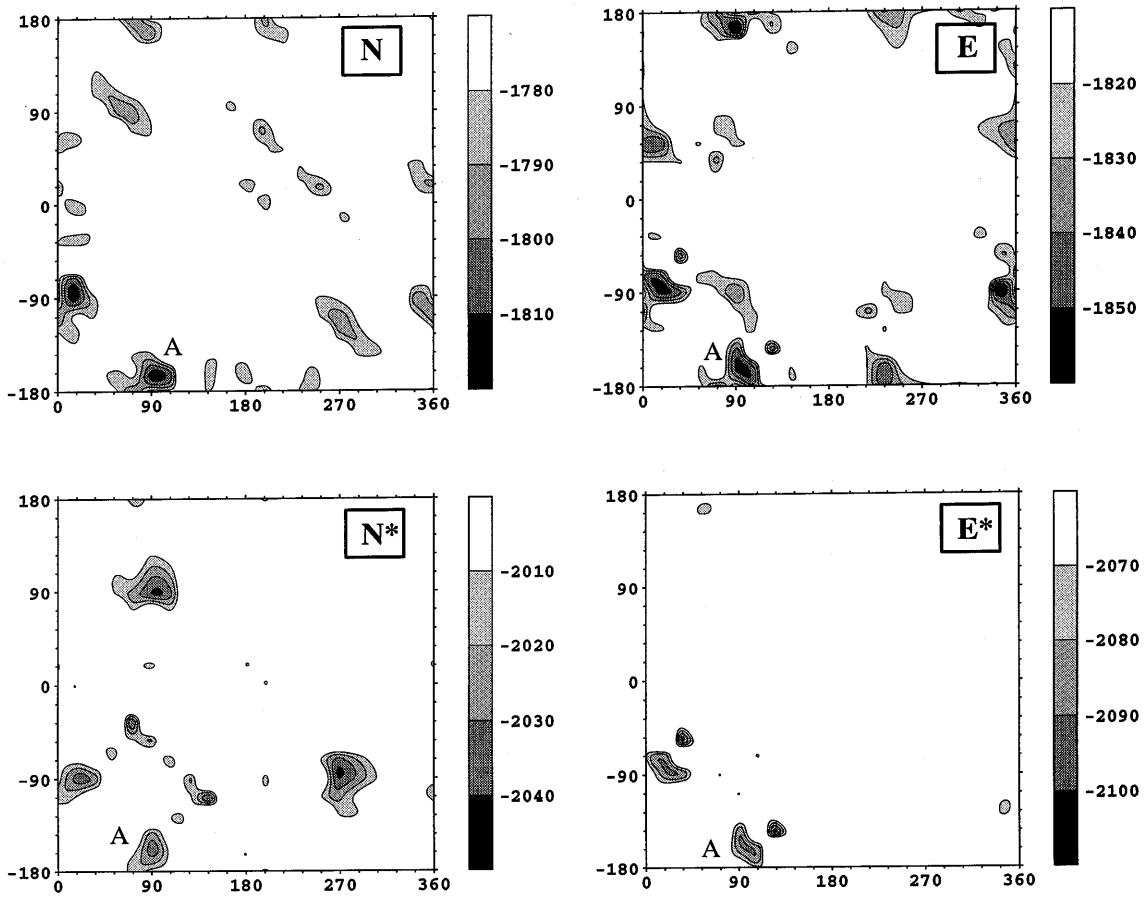

Fig. 2 Potential energy surfaces obtained from the two-body grid search applied to neu/ErbB-2 transmembrane domain (TM) helices for the wild sequence (*top*) and the mutated sequence (*) (*bottom*). *Abscissa*, the rotational angle $\theta 1$ about the helix axis of H1; *ordinates*, the rotational angle $\theta 2$ about the helical axis of H2. The zero value for $\theta 1$ and $\theta 2$ corresponds to the X axis (perpendicular to the helix axis Z) going through the Cα atom of the first residue. Energy contours are plotted at intervals of 10 kJ/mol from the lowest-energy minimum. State A, common for neu and ErbB-2, is the starting structure for the simulations

smallest distance is obtained for the two left-handed structures E2* and N2*, which show regular helices. As expected, the largest distance is observed for E1* and N1, two structures with distorted helices. These distances of closest approach are within the range observed for packed TM helices (0.96 ± 0.19 nm) (Bowie 1997b).

Structure comparison

The root mean square deviation (RMSD) values obtained from the superimposition of the Cα atoms of the two helices (except the Cα termini) ranges from 1.12 to 5 Å. This gives a picture of the diversity of the energy minimized time-averaged structures. The two structures, E2* and N2*, are very similar with a RMSD of 1.12 Å and are close to N3* and DI (Cα RMSD around 2 Å) [DI is the structure previously determined for ErbB-2 TM starting from the lowest energy configuration (Garnier et al. 1997)]. The comparison between all other left-handed coiled coils results in a value about 3 Å that reflects the local distortions of the helices occurring transiently along the simulation. Finally, the right-handed structure E3 differs from the ensemble by about 5 Å.

Peptide helicity

The analysis of the different trajectories was undertaken to detect the presence of CO$i\cdots$ NHi + 5 HBs and the frequency of their appearance served to identify motifs particularly sensitive to α/π helix conversion. HB time series have been systematically plotted when i, $i+5$ HBs were detected at more than 20% of the total duration of the simulation (this threshold value is significant to indicate changes in α helix structure).

Six simulations out of 10 show that the associated TM helices undergo π distortions. The residence time of these HB during the analyzed period are greater than 80%. Figure 4 gives a schematic representation of the two helices showing their location. For the four other simulations the α helix is retained (E3 and N2*), or only one C-terminal i, i + 5HB is detected on one helix (E2 and E2*). This π HB probably results from end effects and is not structurally significant. Generally, helix dis-

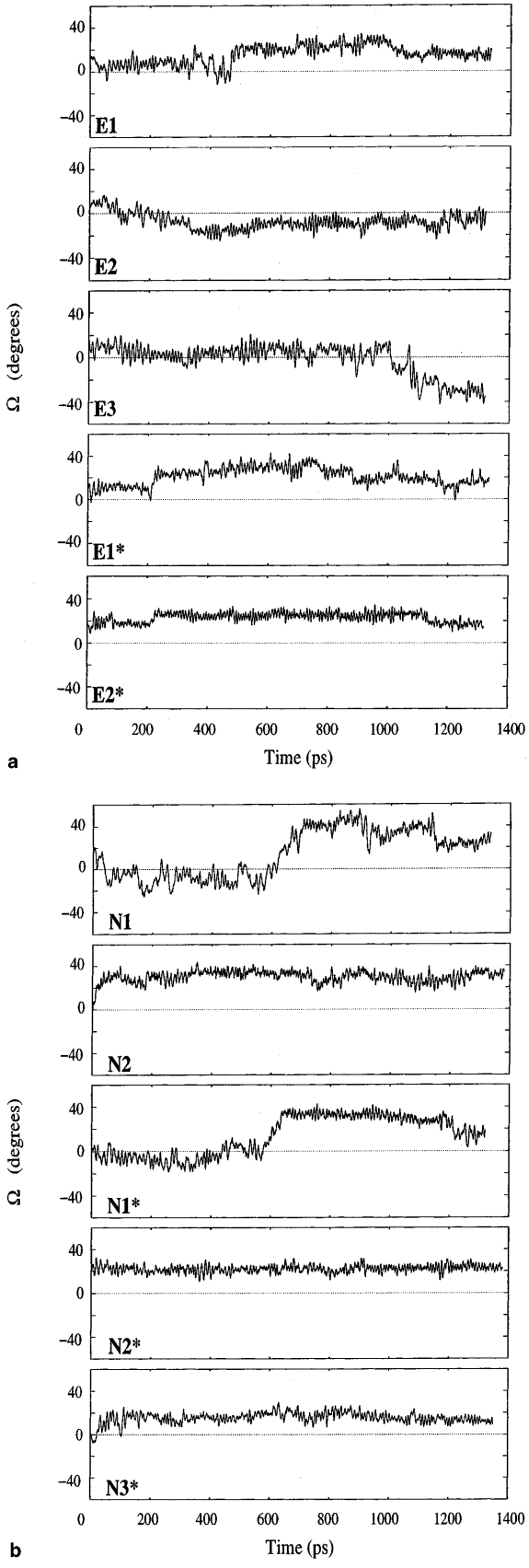

Fig. 3 Time series of the crossing angle Ω (°) along the total length of the simulation for the wild type and the Glu mutated type (*) of ErbB-2 (E) (**a**) and neu (N) (**b**) TM dimers

tortions are unsymmetrical and are observed on both helices or only on one helix.

A first helical distortion appears at the N-terminal side, from Thr2 to Val8, as observed in E1* and N2, giving rise to the exclusion of the CO Ile4 from the α HB network. In E1, the distortion is less pronounced owing to the fact that the COIle4-NHVal8 α HB is only weakened but not broken. A second region sensitive to π alterations, more central, lies over Ile4- Leu13 in N1 and Ile5-Leu13 in N1*, also leading to the exclusion of one carbonyl group pertaining to residue Glu9. In E1, the H2 deformation is shifted and involves the Gly10-Gly18 portion. A third region concerns the C-terminus of the helix where a three π HB portion extending from Gly18/Val18 to Ile25 is often observed. This sequence includes consecutive Val residues and, in the case of neu where four consecutive Val residues are present, the carbonyl group of Val21 is excluded from the HB network. The most extended π portion is observed for E1* with the distorted portion Val14 to Ile25 interrupted by the presence of the Gly22 residue. In that case, the CO groups of Leu17 and Phe21 are excluded from the α HB network.

These results indicate that α helix distortions are sequence dependent and primarily caused by consecutive Val residues. Analysis of inter-helix HBs presented in the following shows that the exclusion of a carbonyl group from HB interactions observed at the terminal end of a π stretch is important for helix association since such a group becomes a potential site for intermolecular HB interactions.

HBs involving side chains

Table 2 summarizes the different type of HB detected during the analysis period. HBs are formed between the polar groups of the side chains and their own backbone (intra-HB) or between the polar groups of two facing side chains or between one side chain and one excluded carbonyl (inter-HB). When the sequence bears the Glu mutation the potentiality of HB interactions increases and the side chain extremities, when favorably oriented at the interface, participate in inter-helix HBs.

For ErbB-2, intramolecular HBs between the Ser and Thr hydroxyl groups are often formed. These same groups also participate in intermolecular HBs. The Ser6 hydroxyl group is found hydrogen bonded to CO Ile4 of the facing helix with a residence time that depends on the accessibility of the carbonyl. In E2* it is observed for a short period in a bifurcated form because the carbonyl group remains involved in the α HB network. In E1 and E1* it is observed for a longer time owing to a greatest accessibility due to its exclusion. The HB and packing

Table 1 Crossing angle values and helix-helix separation of the neu/ErbB-2 transmembrane domain (TM) dimer models. Values are calculated for the energy-minimized time-averaged structures over the last simulation period ranging from 120 ps to 270 ps or 480 ps for N2* (see text). A positive value of Ω indicates a left-handed coiled coil structure and a negative value indicates a right-handed coiled coil structure. DI is the first model proposed for ErbB-2 TM dimer model (Garnier et al. 1997). Inter-helix distances (in nm) are calculated between the geometric centers of seven consecutive Cα atoms considering an α helix of 3.5 residues per turn. The initial distance of separation between parallel helices is 1.07 Å for ErbB-2 and 1.10 Å for neu

	Wild type			Mutated Glu		
ErbB-2	E1	E2	E3	E1*	E2*	DI
Ω (°)	15	−5	−31	15	17	19
d (nm)	0.956	0.998	0.999	1.030	0.945	0.997
neu	N1	N2		N1*	N2*	N3*
Ω (°)	24	31		16	23	13
d (nm)	1.073	0.993		0.989	0.927	0.954

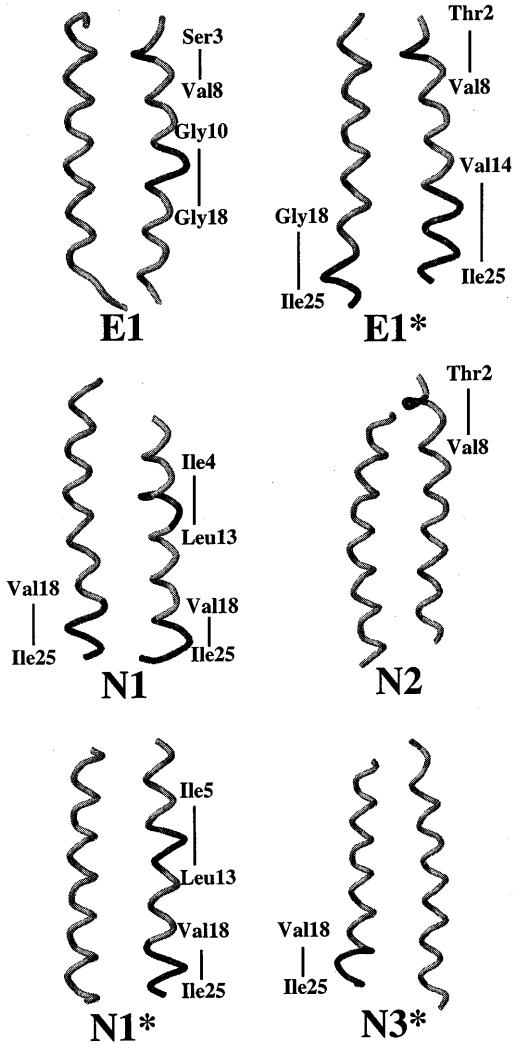

Fig. 4 Schematic view of neu/ErbB-2 TM dimer structures showing distorted helices. Each helix is represented as a tube (H1 at the right, H2 at the left). The π bulge is *darker*. The residues are indicated that limit the π stretch at the N and the C terminus with respectively their CO and NH groups involved in π hydrogen bonds (HBs). All the CO$i\cdots$NH$i+5$ HBs along the π stretch are present at more than 80% of the time of the analyzed period (see Table 2)

angle time series show that this side chain-backbone interaction forces the two helices to slightly reorient, thus allowing inter-HB interactions involving the Glu side chains in the case of the mutated form. The $O\varepsilon_2H$ extremity fluctuates between the facing CO Ile4 or CO Ile5 with HB residence time of 55% and 30%, respectively, indicating an important χ_4 rotational motion. In E2*, helices are undistorted and one HB between the Glu side chain and the facing CO Ile5 is observed at a significant percentage (50%). In that case, crossed Glu-Glu side chain HBs are formed for 25% of the time of the last 120 ps of the simulation.

Similarly, intra- and intermolecular HBs are observed in neu TM dimers. The Thr7 hydroxyl group is very frequently hydrogen bonded to the CO of Phe3 of its own helix and in some cases this interaction is almost symmetric. The Thr2 side chain is engaged in inter-helix HBs with the facing CO Ile4 and CO Ile5 (detected in N2) or, more often, with the carbonyl of the first N-terminal residue of H2 (detected in N1*, N2*, and N3). As observed for ErbB-2, the two Glu side chains are hydrogen bonded through their extremities (HB almost symmetrical in N1*) or only one Glu side chain interacts with the facing CO Ile5 still involved in the helical HB pattern through a bifurcated HB. Glu-Glu interactions are favored by a reorientation of the two helices induced by helical distortions as shown in Fig. 5.

For the parallel helix association obtained in E2, the absence of inter-helix HBs involving side chains all along the simulation is to be noted. For E3, when the helices wrap in the right sense, HB interactions are established for short laps of time but are not responsible for the transition from the left to the right helix packing observed at about 1000 ps. This event is essentially driven by van der Waals forces.

Dimer stability

The stability of the different models is expressed as the sum of the intramolecular energy of individual helices and the intermolecular energy between the two helices. The results are given in Table 3 and are analyzed in relation to the monomer helicity and inter-helix HBs.

Table 2 Hydrogen bonds (HBs) in neu/ErbB-2 TM dimer models. Intra and inter hydrogen bonds involving side chains are detected during the final period of the simulations given in parentheses. HB presence time is given as a percentage of the time of this period

Simulations		N1 (1155–1335 ps)	N2 (1200–1380 ps)	N1* (1200–1320 ps)	N2* (900–1380 ps)	N3* (1200–1350 ps)
Intra HB H1	Thr7OγH-Phe3CO	30%	38%	62%	24%	29%
	Thr7OγH-Ile4CO	–	–	–	–	20%
Intra HB H2	Thr7OγH-Phe3CO	47%	–	24%	32%	–
Inter helix HB H1-H2	Thr2OγH-Val1CO	–	–	95%	68%	98%
	Thr2OγH-Ile4CO	–	27%	–	–	–
	Thr2OγH-Ile5CO	–	68%	–	–	–
	Glu9Oε_2H-Glu9Oε_1	–	–	39%	30%	–
	Glu9Oε_2H-Glu9Oε_2	–	–	–	27%	–
	Glu9Oε_2H-Ile5CO	–	97%	–	25%	85%
	Glu9Oε_1-Glu9Oε_2H	–	–	50%	–	–
		E1 (1065–1335 ps)	E2 (1200–1320 ps)	E3 (1200–1320 ps)	E1* (1155–1335 ps)	E2* (1200–1320 ps)
Intra HB H1	Thr2OγH-Ser6Oγ	66%	–	–	82%	29%
	Ser3OγH-Thr2CO	21%	22%	26%	–	–
	IIe5NH-Ser3Oγ	40%	–	–	37%	–
	Thr2OγH-Thr2CO	21%	–	27%	–	–
Intra HB H2	Ser6OγH-Leu1CO	55%	–	26%	–	–
Inter helix HB H1-H2	Ser6OγH-Ile4CO	72%	–	–	97%	36%
	Glu9Oε_2H-Glu9Oε_2	–	–	–	–	25%
	Glu9Oε_2H-Ile4CO	–	–	–	55%	–
	Glu9Oε_2H-Ile5CO	–	–	–	30%	50%
	Leu1CO-Leu1NH	–	97%	34%	92%	69%
	Thr2Oγ-Thr2OγH	90%	–	–	–	–

Van der Waals energies of individual helices range from −591 to −668 kJ/mol for ErbB-2 and from −558 to −660 kJ/mol for neu. The origin of these variations mainly comes from the internal structure of the helices. When the helices keep the α HB network practically all along the chain (E2*, N2*), they differ only by a few kJ/mol in stability. When the α HB network is broken and replaced by π HB, the van der Waals stability increases. This is illustrated in Fig. 6 for N1*. On the other hand, the presence of local structural defaults tends to destabilize electrostatic interactions. These results have been already described for isolated helices (Duneau et al. 1997). π HB formation releases steric constraints induced primarily by Val side chains and weakens electrostatic interactions by the presence of bifurcated HBs at the junction of the α and π HB networks and by the exclusion from the HB network of CO groups.

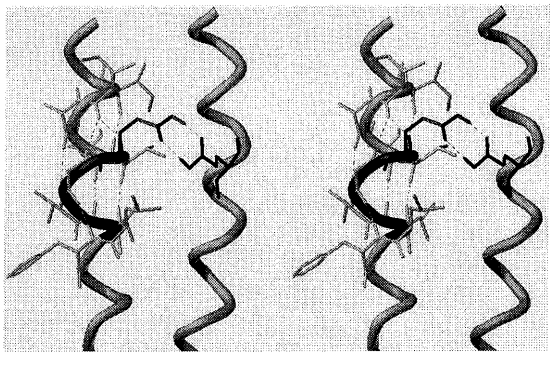

Fig. 5 Stereo view of the symmetric HBs between the two Glu side chains observed in the neu TM dimer (N1*). The backbone is represented by a *tube* (H1 at the right, H2 at the left). The local π distortion on H2, from Ile4 to Phe14 (from top to bottom), is *shaded*

Van der Waals interactions between the two helices are the main component for dimer stability and the difference in energy depends upon the monomer structure. As an example, the intermolecular energy of the two left-handed coiled-coil structures of the mutated ErbB-2 TM dimer differ by about 30 kJ/mol, the energy being lower when the helices keep the α structure. Another interesting result is that, for the wild ErbB-2 helices, left-handed interactions of are much favorable than parallel or right-handed interactions.

Obviously the differences in van der Waals interactions reflect the differences in the mode of packing resulting from the relative position of the two helices and local backbone distortions. This is shown by comparing N1 and N2. In both cases the two helices that are shifted along the helical axis lose packing interactions at the their N-terminal extremities and N1, with the most distorted helices shows inter-helix interactions 50 kJ/mol lower than in N2.

Another factor that contributes to reinforce the dimer stability is the formation of inter-helix HBs, particularly those involving side chain-backbone interactions which are correlated to an important increase (several tens in kJ/mol) in electrostatic energies. An example of a gap in energy is given for N2 (Fig. 7a), when the inter-helix HB

Table 3 Energies (in kJ/mol) of the neu/ErbB-2 TM dimer structures. Values are averaged over the analyzed period of the simulation (given in Table 2)

Potential energy	Simulations	Electrostatic energy			van der Waals energy		
		Intra H1	Inter H1-H2	Intra H2	Intra H1	Inter H1-H2	Intra H2
E1 (1065–1335 ps)	−545	−352	−36	−356	−595	−335	−619
E2 (1200–1320 ps)	−520	−345	14	−395	−613	−286	−608
E3 (1200–1320 ps)	−482	−362	29	−390	−593	−287	−606
E1* (1155–1335 ps)	−798	−445	−41	−451	−646	−303	−668
E2* (1200–1320 ps)	−762	−460	−18	−472	−591	−339	−627
N1 (1155–1335 ps)	−374	−361	30	−319	−640	−258	−645
N2 (1200–1380 ps)	−412	−377	−10	−321	−594	−304	−620
N1* (1200–1320 ps)	−640	−466	−15	−420	−620	−283	−660
N2* (900–1380 ps)	−645	−472	11	−456	−617	−322	−615
N3* (1200–1350 ps)	−650	−459	−12	−447	−640	−312	−558

between Thr2 and CO Ile5 is formed. The HB transition between CO Ile5 and CO Ile4 has no drastic effect on the stability. This type of side chain-backbone interaction permits a close approach of the two helices and induces the formation of other inter-helix HBs, as revealed by the time series. The major result is that the Glu mutation leads to a strong stability of the dimers both for neu and ErbB-2 (Fig. 7b).

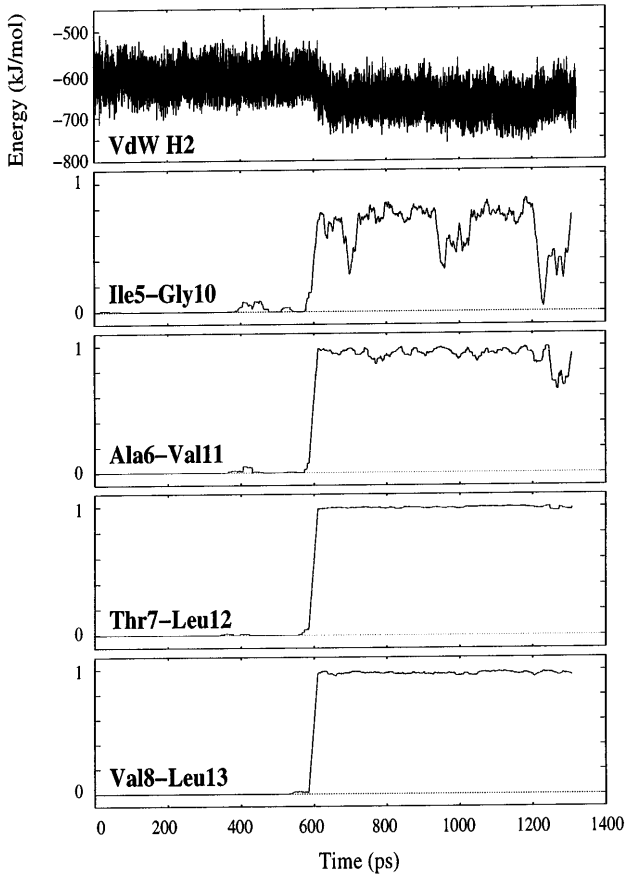

Fig. 6 Time evolution of intramolecular van der Waals energies illustrating the stabilizing effect induced by π helix formation. In the neu TM dimer N1*, the four π HBs at the N-terminal side on one helix correlate with a decrease in energy. This same deformation is correlated to the change in helix packing going from a parallel helix arrangement to a left-handed helix arrangement at about 600 ps (see Fig. 3b)

Helix packing

We now examined our results in terms of the two principal models that have been developed to characterize how helices are packed. The first one is the "knobs-into-holes" (K/H) model (Crick 1953) that describes residues of one helix (knobs) at the center of the interface that fit into cells (holes) formed by four neighboring residues in the other helix. In such a model the residues form a repeated motif of seven amino acids $(abcdefg)_n$. In the case of parallel helix pairs, the interface is characterized by residues a′ and residues d′ on one helix that pack against residues a, d, d, g and d, a, a, e of the neighbor helix, respectively (Langosch and Heringa 1998).

Application of the K/H model to our unsymmetrical MD structures necessitates consideration of the two helices individually to respect this rule. Under this assumption, the helix packing of E2* and N2* conforms to the K/H model (Fig. 8a). Close contacts are observed for the total length of the structures except at the N- and C-termini, which are slightly distorted. For some structures with distorted helices the K/H packing can be described by introducing discontinuities in the heptad repeat (Brown et al. 1996). The unwinding induced by one additional residue in a helix turn leads to a shift of a heptad of one residue. E1 with the central π deformation on H2 clearly illustrates this effect. Contacting residues are identical to those observed for E2* in the first half of the structure and the effect of the π bulge over Gly10-Gly18 is to skip Val15, which is replaced by Val16 at position d. For the second half of the structure, helix packing is symmetric and residues Gly10 and Gly18 on H2 are shifted out of the interface. Tight contacts are observed all along the helix-helix interface, stronger than in E2* (Fig. 8a).

In the case of N3*, for which a distortion affects the C-terminus on H1, the regularity of the packing is destroyed (not shown). The cavities formed by the two last cells are widened and each can accommodate two facing side chains of H2 (Leu15, Val19 and Val19, Ile23). This

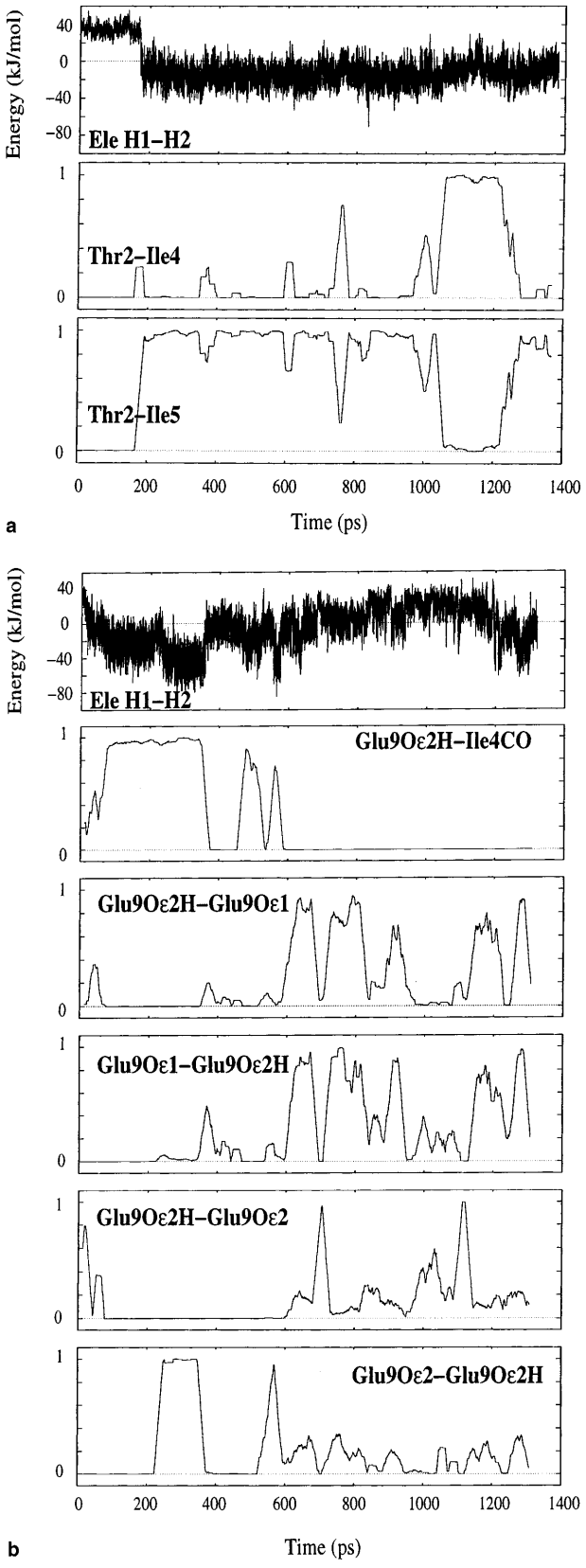

Fig. 7 Time evolution of electrostatic energies between the two helices: **a** for simulation N2 of the wild neu TM dimer, showing the large increase in energy induced by HB formation between the hydroxyl group of Thr2 and the carbonyl group of the facing Ile5 residue; during the simulation this HB is broken and CO Ile4 replaces CO Ile5; **b** for simulation N1* of the mutated neu TM dimer, showing the effect of side chain-backbone and side chain-side chain HB interactions involving the Glu mutant

structure is exemplified by an intermediate state between the regular K/H packing and that obtained after a skipped residue.

The other structures, with shifted helices or with more important helical distortions, are better described by the "ridges-into-grooves" (R/G) model proposed by Chothia et al. (1981). The R/G pattern describes ridges formed by residues with sequential spacing 1, 4, or 3 in the first helix that fit into grooves formed by residues with sequential spacing 4 in the second helix. This 3-4 basic packing type that optimizes at a crossing angle of $+23°$ includes that of the K/H. It is easily applied to N2* as shown in Fig. 8b (this pattern is identical to E2*), but can be softened to describe the organization of interfacial residues of noncanonical helices.

The graphical view of the averaged minimized structures, using space filling representation for the Cβ atoms of the contacting residues, was very helpful to describe most of the structures by a slightly varied 3-4 packing type. The R/G model illustrates particularly well the effect of the helix shift along the axis by the displacement of the ridges of one helix into the grooves of the facing helix. This is shown for N2 (Fig. 8b) by the exclusion of the first residues of the grooves on H2 and the appearance of new residues at the tail. The distortion at the N-terminus of H2 does not affect the regularity of the 3-4 spacing. Such a model can also be applied to E1*, N1, and N1, for which the conjugated effect of the distortions within the helices results in modifying the composition of the ridges (not shown).

Finally, parallel and right-handed interactions found in E2 and E3, respectively, do not conform to the K/H or the R/G models.

To summarize, Fig. 9 gives a representation of the interface observed in N2*.

Discussion

Methodology and its limitation

Molecular modeling has proved its relevance to successfully predict the structure of the coiled-coil assembly. An automated model building procedure (Nilges and Brünger 1991) was used to predict the structure of the dimerization domain of GCN4 leucine zipper and glycophorine A (Treutlein et al. 1992). This protocol based on a simulated annealing (SA) approach via restrained MD simulations, has been largely applied to modeling single transmembrane helices and bundles of transmembrane helices (Sankararamakrishnan and Sansom 1995a, b; Kerr et al. 1996; Biggin et al. 1997; Tieleman

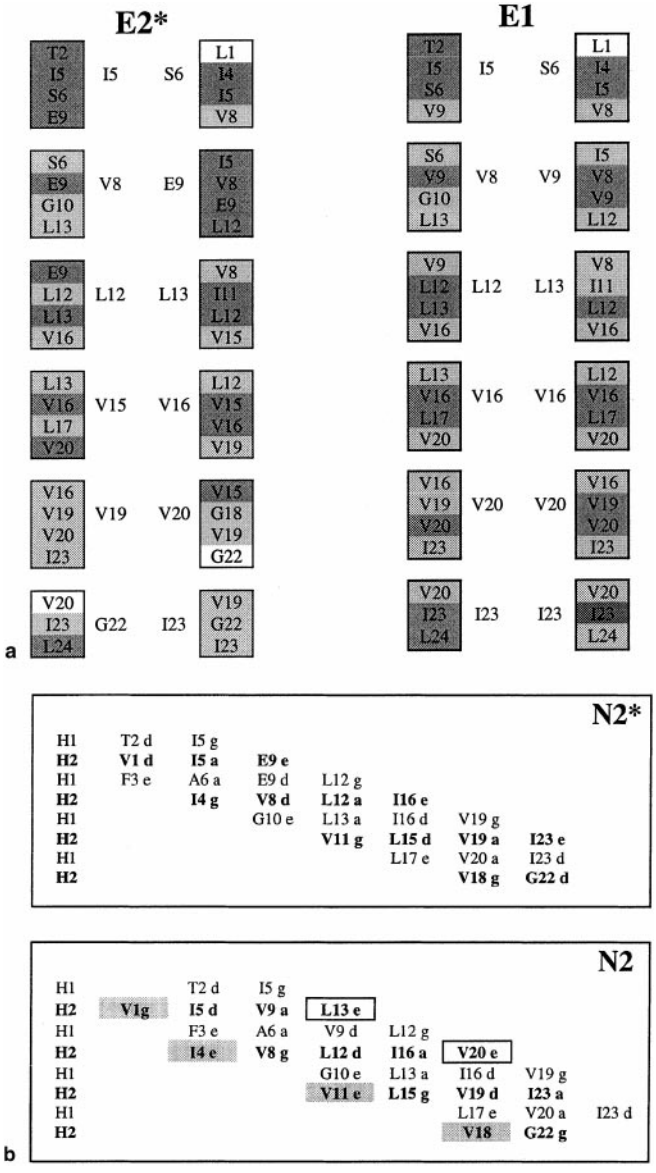

Fig. 8 **a** Knobs-into-holes packing observed in ErbB-2 TM dimer models: side chains of one helix (knobs) protrude into cells (holes) formed by four residues of the facing helix. Contacting residues, with three atoms within 0.06 nm of the sum of their van der Waals radii with three facing atoms, are *boxed in dark gray*. "Soft" contacting residues (see text for criteria) are *boxed in light gray*. When atomic distances are greater than 0.65 nm the residues are *boxed in white*. For model E2* of the oncogenic ErbB-2 TM dimer the helix-helix interface is unsymmetrical. Model E1 of the wild ErbB-2 TM dimer exemplifies the heptad disruption induced by the π helix portion over Gly10 to Gly18, leading to a symmetrical interface. **b** Ridges-into-grooves packing model applied to the neu TM dimer N2* and N2. In model N2 the shift of the two helices along their axis results in a shift of the ridges of one helix onto the grooves of the facing helix. Compared to N2*, residues disappear from the helix-helix interface (*boxed in gray*) and residues moved within the interface (*boxed in white*)

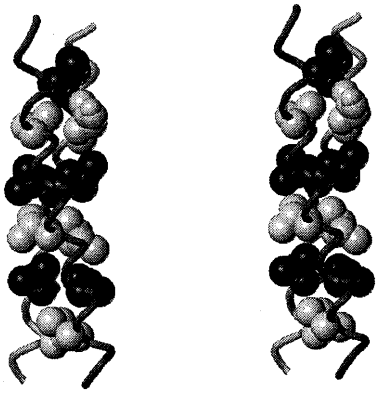

Fig. 9 Stereo view of the helix-helix interface observed in neu TM dimer (model N2*). Helical backbones are represented as a tube (H1 *gray* and H2 *dark gray*). Residues in position a (*dark gray*) and in position d (*gray*) (see Fig. 7b) within the interface are represented in a space filling model

et al. 1999). The procedure starts from α helical Cα templates incorporating distance restraints such as HBs and intra-helix separation to ensure the generation of homogenous ensembles of structures.

Another approach based on the two-stage model of membrane protein folding (Popot and Engelman 1990) uses complete search methods that sample all possible helix interactions. Such a global search succeeds in predicting the structure of the pentameric transmembrane domain of phospholamban (Adams et al. 1995) and to improve the dimer structure of glycophorin A (Adams et al. 1996). Less sophisticated than the SA/MD procedure, the global search of interacting helices improves the sampling of all possible packing interactions between helices and a careful consideration of mutagenesis data may be a reliable indicator of model correctness.

We have used a similar approach to predict the left-handed structure of the wild and oncogenic types of the ErbB-2 TM helices (Garnier et al. 1997) and this first model was closely related to the oncogenic form of the neu TM dimer model suggested from experimental data (Smith et al. 1996).

The present work goes further in the structure prediction of the transmembrane domain dimerization for two members of the erbB family, neu and ErbB-2 (Sajot et al. 1999). The study concerns one particular configuration, issued from a global search method for favorable orientations of parallel helices. This low-energy configuration is identical for the wild and the oncogenic type of the two TM receptors and exhibits the mutation site within the helix-helix interface. From a large sample of configurations obtained over about 13 ns of in vacuo MD simulations we demonstrate that uncoiled helices of neu/ErbB-2 TM preferentially wrap in left-handed interactions.

The global search was undertaken without any assumption and MD refinement was carried out without any structural constraints. This strategy explains why substantial distortions from helical geometry, particularly at the terminal ends, are observed, contrary to the structures of the helices obtained from SA/MD (Biggin et al. 1997).

The main limitation of our approach is that MD simulations are performed without a membrane environment. Nevertheless, as already discussed (Duneau et al. 1996, 1997), the vacuum approximation is reasonable owing to the fact that the core of the membrane is a highly hydrophobic medium with a low dielectric constant. This approximation, used by other authors to describe models for dimer structure (Treutlein et al. 1992; Lemmon et al. 1994), is supported by our recent results showing that isolated helices simulated in a vacuum or with an explicit membrane environment explore the same conformational space (Duneau et al. 1999a). The main factors that drive TM dimerization come from the hydrophobic side chains that must be docked with their neighbors to optimize helix packing. If the role of lipid-peptide interactions cannot be ignored it is certainly not specific for helix-helix association. Consequently, one may suppose that structural dimer features found within a vacuum are close to those adopted in a membrane environment.

A few experimental have studies addressed the structure of neu and neu* transmembrane domains, demonstrating the α helical structure of a short modified fragment of the neu TM domain (Gullick et al. 1992) and of the complete TM domain that extends through the membrane interface (Smith et al. 1996; Burke and Stern 1998). Our MD simulations show that TM helices undergo π deformations. We have previously shown that, in isolated helices, occurrence of these deformations is mainly caused by the presence of successive β-branched residues (Duneau et al. 1997). The HB analyses indicate that the sites sensitive to deformations in associated helices are identical to those found in isolated helices. This suggests that this sequence-dependent property might play a role in the association process. It is worth noting that similarly deformed helices are observed in transmembrane proteins (Henderson et al. 1990; Kuhlbrandt et al. 1994; Deisenhofer et al. 1995; McDermott et al. 1995; Grigorieff et al. 1996; Tsukihara et al. 1996; Xia et al. 1997). In addition, the HB formed between a Trp residue on one helix (helix VIII of the subunit I) and a Gly carbonyl group of the facing helix (subunit VIIa) within the dimer interface of cytochrome *c* oxidase (Tsukihara et al. 1996) seems determinant for the dimer stability. This side chain-backbone HB interaction is induced by local π helix structure, as described in our MD models.

Coiled coil structures

Two experimental studies (Smith et al. 1996; Burke and Stern 1998) strongly suggest that dimerization might be achieved by left-handed coiled-coil or parallel helical interactions but no structural detail is given for their association.

The present MD simulations provide important structural information by demonstrating that, from an unbiased protocol, neu/ErbB-2 TM helices prevail in left-handed interactions at about $+20°$. Only two simulations relative to the wild ErbB-2 sequence fail, one describing parallel interactions, the other describing right-handed interactions. However, an important point to underline is that the other continuation of this last simulation over 10 ns converges to helices crossed at a left packing angle (data not shown). Then, it is highly probable that all the simulations would converge to the same left-handed coiled coil provided that the simulation is sufficiently long. This study also shows the necessity to perform multiple simulations to evidence structural features.

All our models describe unsymmetrical structures. Asymmetry comes from the starting point for MD refinement for which the mutation site is not symmetrically positioned within the interface. Even if the simulation is pursued over 10 ns, as mentioned above, it does not converge on a symmetric interface. One may suppose that the two helices are initially too close to each other, thus preventing the facing side chains from crossing over to reach symmetry. Symmetry could be achieved by starting from an initial symmetric structure, but this does not conform with our ab initio strategy of global search.

Another result of importance is that left-handed interactions conform to the R/G model used to describe the helix packing and more precisely that the dimer models with helices close to the α structure conform to the K/H side chain packing. This model, that appears as the central determinant of coiled coil structures, well exemplified by the GCN4 leucine zipper helix packing (O'Shea et al. 1991), is generally used to describe associated TM helices. In addition, we have shown that, in some cases, π deformations on helices do not disrupt the K/H packing and allow to partially retrieve the symmetry for the contacting surface.

Energy variations between the different structures show that the Glu residue present at the helix-helix interface contributes to a large increase in stability. Van der Waals interactions between the two helices are more favorable than those observed for the wild-type dimers and electrostatic interactions are generally lower. Negative values of electrostatic energy between the helices of the wild dimers reported in few cases come from inter hydrogen bonding involving the polar side chains of Ser and Thr residues that flank the TM region.

Considering the three types of helix winding found for wild ErbB-2 TM dimer, we have shown that left-handed interactions allow closer contacts than observed in a parallel or a right-handed arrangement. The helix-helix separation varies according to the volume of the contacting side chains and the locations of backbone distortions along the helix. These three different models obtained for the wild ErbB-2 dimer could be interpreted as a weaker specificity than for the mutated sequence, but this might be smoothed out when embedded in a bilayer model.

The energy of the system alone is not sufficient to ensure the correctness of the models. Experimental

observations validate the presence of hydrogen bonding between the two Glu residues in the mutated TM dimer, but potential hydrogen bonds to lipids and water certainly compete, particularly at the membrane interface (Duneau et al. 1999b; Forrest et al. 1999). Also, hydrophobic interactions involving the helix faces exposed to the aliphatic tails of the lipids, which are missing in our approach, may contribute to modulate dimer stability.

The effect of hydrogen bonding is to hold the TM dimer in place in the bilayer but, before we quantify the relative contributions of hydrogen bonding and hydrophobic interactions to TM helix/bilayer interactions, further MD studies of TM helices are required (Biggin and Sansom 1999).

Dimer interface

By constructing a consecutive series of cysteine substitutions in the neu juxtamembrane domain, Burke and Stern (1998) identify a productive inter-receptor interface formed by helical contacts distributed along the juxtamembrane domain and the transmembrane domain. Considering a helix with 3.5 residues per turn, the subset of transforming substitutions spreads over 250° about the helix axis, and nontransforming substitutions define a small region out of the receptor-receptor interface. On the basis of these data, the authors proposed a helix interface (noted B) involving residue Val656 at position d (and d′) and residue Thr657, aligned with Glu664, at position e (and e′) [heptads are designated a through g from the amino terminus (Langosch and Heringa 1998)]. This model respects the ionic interactions at the juxtamembrane interface at positions g and e, but appears incompatible with inter-helix HBs between the two Glu side chains or with crossed HBs between Glu and the facing Ala 661 as presumed by Sternberg et Gullick (1989) except assuming major helical defaults.

A comparison of this interface (B) with that described in our MD models E2* (D) is shown in Fig. 10a. The helical wheel representation shows that the H2 interacting face matches with B and that the H1 interacting face defines the D interface. One may remark that the D interface corresponds to a dimer model which places, according to cysteine transforming activity, residue Thr657 at position d (and d′) aligned with Glu664, and residue Ala 661 at position a (and a′) that might be more favorable for the presumed HB interactions. Interfaces B and D spread over 150° each and are superimposed over 50°. Interestingly, taken together they perfectly match the region defined by the subset of strongly transforming and intermediate transforming substitutions of Burke and Stern (1998). One may remark that the helix face (F), predicted unfavorable for dimerization from cysteine mutagenesis analysis, is located outside the dimer interface defined in our model E2*.

If we consider the other left-handed model E1, less regular than the previous E2*, it can be remarked that

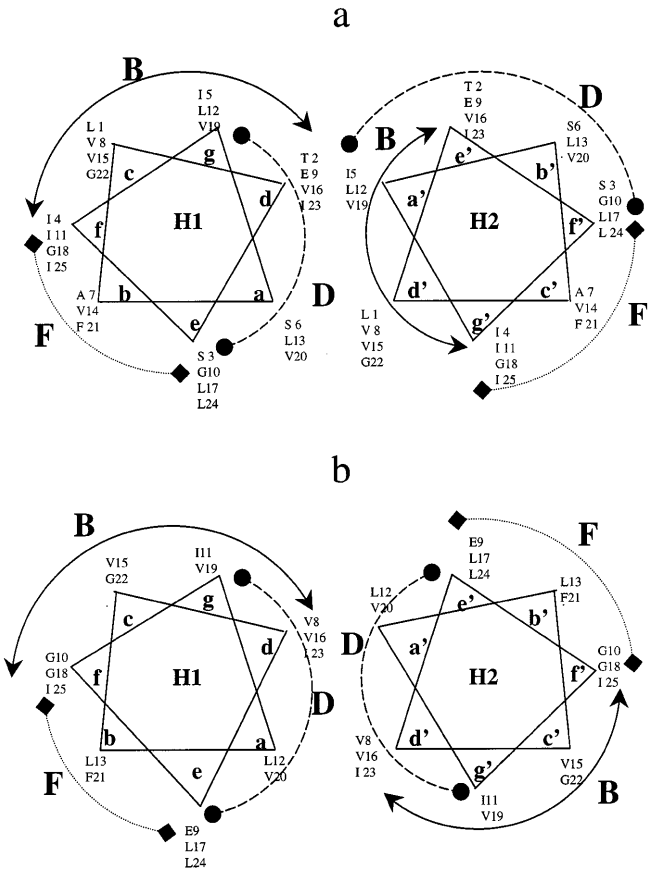

Fig. 10a, b Helical wheel representation of the ErbB-2 TM dimer interface. **a** In model E2*, relative to the oncogenic type the unsymmetrical interface is composed of B [the helix face proposed by Burke and Stern (1998)] and of D. This helix face D corresponds to another activating mutation T657C at position d within the interface (see text). B and D have a common region over 50° about the helical axis. F is the helix face forbidden for dimerization according to mutagenesis studies. **b** In model E1, a symmetric interface is defined in the second half of the structure, through the effect of a π distortion that occurs on one helix (H2)

the same unsymmetrical interface (a combination of B and D) is defined for the first half of the structure and that the central π deformation on one helix, that induces a rotation of 100°, restores the symmetric D interface for the second half (Fig. 10b). One may imagine a similar rotation of 100° of the second helix that would restore the symmetrical B interface. This observation raises the question of the functional role of helical deformations.

For the other MD models the same combination of B and D interfaces is found, with minor variations according to helix deformations or shift of helices.

Another comment concerns the conservation of the Ala661, Val663, Glu664, and Gly665 motif that encompasses the VEG triplet necessary for full transforming activity according to the mutational analysis of the neu TM region (Cao et al. 1992). Considering the symmetrical dimeric interface proposed by Burke and Stern (1998), only the two residues Val663 and Glu664 are present within interface and the third one, Gly665, is

outside. In our unsymmetrical model the four residues are present within the D interface and, in addition, all the residues conserved between the neu and ErbB2 TM sequences are facing each other.

Conclusion

Our molecular modeling study gives insight into the neu/ErbB-2 transmembrane helix association process. However, although mutagenesis studies and theoretical models describe common features of the TM dimer interface, all the results of transforming activities are not totally well interpreted. The possibility of hydrogen bond rupture of the helical network, that makes appear potential sites for intermolecular interactions, complicates the analysis. At this stage of knowledge of neu/ErbB-2 dimerization, left-handed interactions of the transmembrane domains are highly probable, but essential residues required for activity are still undefined. Further modeling studies are under investigation to progress in this field of RTK signal transduction.

Acknowledgements We are grateful to Dr. Norbert Garnier for providing us with the initial coordinates of the ErbB-2 TM and Dr. Daniel Genest for a critical reading of the manuscript.

References

Adams PD, Arkin IT, Engelman DM, Brünger AT (1995) Computational searching and mutagenesis suggest a structure for the pentameric transmembrane domain of phospholamban. Struct Biol 2: 154–162

Adams PD, Engelman DM, Brünger AT (1996) Improved prediction for the structure of the dimeric transmembrane domain of glycophorin A obtained through global searching. Proteins 26: 257–261; erratum (1997) Proteins 27: 132

Bargmann CI, Weinberg RA (1988) Oncogenic activation of the neu-encoded receptor protein by point mutation and deletion. EMBO J 7: 2043–2052

Bargmann CI, Hung MC, Weinberg RA (1986) Multiple independent activations of the neu oncogene by a point mutation altering the transmembrane domain of p185. Cell 45: 649–657

Berendsen HJC, Postma JPM, van Gunsteren WF, Dinola A, Haak JR (1984) Molecular dynamics with coupling to an external bath. J Chem Phys 81: 3684–3690

Biggin PC, Sansom MSP (1999) Interactions of the alpha helices with lipid bilayers: a review of simulations studies. Biophysical Chemistry 76: 161–183

Biggin PC, Breed J, Son HS, Sansom MSP (1997) Simulations studies of alamethicin-bilayer interactions. Biophy J 72: 627–636

Bowie JU (1997a) Helix packing angle preferences. Nat Struc Biol 4: 915–917

Bowie JU (1997b) Helix packing in membrane proteins. J Mol Biol 272: 780–789

Brandt-Rauf PW, Rackovsky S, Pincus MR (1990) Correlation of the structure of the transmembrane domain of the neu oncogene-encoded p185 protein with its function. Proc Natl Acad Sci USA 87: 8660–8664

Brown JH, Cohen C, Parry DA (1996) Heptad breaks in a helical coiled coils: stutters and stammers. Proteins Struct Funct Genet 26: 134–145

Burke CL, Stern DF (1998) Activation of neu (ErbB-2) mediated by disulfide bond-induced dimerization reveals a receptor tyrosine kinase dimar interface. Mol Cell Biol 18: 5371–5379

Burke CL, Lemmon MA, Coren BA, Engelman DM, Stern DF (1997) Dimerization of the p185neu transmembrane domain is necessary but not sufficient for transformation. Oncogene 14: 687–696

Cao H, Bangalore L, Bormann BJ, Stern DF (1992) A subdomain in the transmembrane domain is necessary for p185neu* activation. EMBO J 11: 923–932

Chen LI, Webster MK, Meyer AN, Donoghue DJ (1997) Transmembrane domain sequence requirements for activation of the p185 c-neu receptor tyrosine kinase. J Cell Biol 137: 619–631

Chothia C, Levitt M, Richardson D (1981) Helix to helix packing in proteins. J Mol Biol 145: 215–250

Coussens L, Yang-Feng TL, Liao YC, Chen E, Gray A, McGrath J, Seeburg PH, Libermann TA, Schlessinger J, Francke U (1985) Tyrosine kinase receptor with extensive homology to EGF receptor shares chromosomal location with neu oncogene. Science 230: 1132–1139

Crick FHC (1953) The packing of α helices: simple coiled-coils. Acta Crystallogr 6: 689–697

Deisenhofer J, Epp O, Sinning I, Michel H (1995) Crystallographic refinement at 2.3 Å resolution and refined model of the photosynthetic reaction centre from *Rhodopseudomonas viridis*. J Mol Biol 246: 429–457

Dunbrack RL, Karplus M (1993) Backbone-dependent rotamer library for proteins. Application to side-chain prediction. J Mol Biol 230: 543–574

Duneau JP, Genest D, Genest M (1996) Detailed description of an α helix $\rightarrow \pi$ bulge transition detected by molecular dynamics simulations of the p185c-erbB2 V659G transmembrane domain. J Biomol Struct Dyn 13: 753–769

Duneau JP, Garnier N, Genest M (1997) Insight into signal transduction: structural alterations in transmembrane helices probed by multi-1 ns molecular dynamics simulations. J Biomol Struct Dyn 15: 555–572

Duneau JP, Crouzy S, Chapron Y, Genest M (1999a) Dynamics of the transmembrane domain of the ErbB-2 receptor. Theor Chem Acc 101: 87–91

Duneau JP, Crouzy S, Garnier N, Chapron Y, Genest M (1999b) Molecular dynamics simulations of the ErbB-2 transmembrane domain within an explicit membrane environment: comparison with vacuum simulations. Biophys Chem 76: 35–53

Forrest LR, Tieleman DP, Sansom MSP (1999) Defining the transmembrane helix of M2 protein from influenza A by molecular dynamics simulations in a lipid bilayer. Biophys J 76: 1886–1896

Garnier N, Genest D, Hebert E, Genest M (1994) Influence of a mutation in the transmembrane domain of the p185c-erbB2 oncogene-encoded protein studied by molecular dynamics simulations. J Biomol Struct Dyn 11: 983–1002

Garnier N, Genest D, Duneau JP, Genest M (1997) Molecular modeling of c-erbB2 receptor dimerization: coiled-coil structure of wild and oncogenic transmembrane domains. Stabilization by interhelical hydrogen bonds in the oncogenic form. Biopolymers 42: 157–168

Grigorieff N, Ceska TA, Downing KH, Baldwin JM, Henderson R (1996) Electron-crystallographic refinement of the structure of bacteriorhodopsin. J Mol Biol 259: 393–421

Gullick WJ, Bottomley AC, Lofts FJ, Doak DG, Mulvey D, Newman R, Crumpton MJ, Sternberg MJ, Campbell ID (1992) Three dimensional structure of the transmembrane region of the proto-oncogenic and oncogenic forms of the neu protein. EMBO J 11: 43–48

Gunsteren WF van (1987) GROMOS, Groningen molecular simulation system. BIOMOS Biomolecular Software, Groningen, The Netherlands

Henderson R, Baldwin JM, Ceska TA, Zemlin F, Beckmann E, Downing KH (1990) Model for the structure of bacteriorhodopsin based on high-resolution electron cryo-microscopy. J Mol Biol 213: 899–929

Hynes NE, Stern DF (1994) The biology of erbB-2/neu/HER-2 and its role in cancer. Biochim Biophys Acta 1198: 165–184

Jenkins BJ, D'Andrea R, Gonda TJ (1995) Activating point mutations in the common beta subunit of the human GM-CSF, IL-3 and IL-5 receptors suggest the involvement of beta subunit dimerization and cell type-specific molecules in signalling. EMBO J 14: 4276–4287

Kerr ID, Son HS, Sankararamakrishnan R, Sansom MS (1996) Molecular dynamics simulations of isolated transmembrane helices of potassium channels. Biopolymers 39: 503–515

Kuhlbrandt W, Wang DN, Fujiyoshi Y (1994) Atomic model of plant light-harvesting complex by electron crystallography. Nature 367: 614–621

Langosch D, Heringa J (1998) Interaction of transmembrane helices by a knobs-into-holes packing characteristic of soluble coiled coils. Proteins Struct Funct Genet 31: 150–159

Lemmon MA, Treutlein HR, Adams PD, Brünger AT, Engelman DM (1994) A dimerization motif for transmembrane alpha-helices. Nat Struct Biol 1: 157–163

Lemoine NR, Staddon S, Dickson C, Barnes DM, Gullick WJ (1990) Absence of activating transmembrane mutations in the c-erbB-2 proto-oncogene in human breast cancer. Oncogene 5: 237–239

Lofts FJ, Hurst HC, Sternberg MJ, Gullick WJ (1993) Specific short transmembrane sequences can inhibit transformation by the mutant neu growth factor receptor in vitro and in vivo. Oncogene 8: 2813–2820

Longo N, Shuster RC, Griffin LD, Langley SD, Elsas LJ (1992) Activation of insulin receptor signaling by a single amino acid substitution in the transmembrane domain. J Biol Chem 267: 12416–12419

McDermott G, Prince SM, Freer AA, Hawthornthwaite-Lawless AM, Papiz MZ, Cogdell RJ, Isaacs NW (1995) Crystal structure of an integral membrane light-harvesting complex from photosynthetic bacteria. Nature 374: 517–521

Miloso M, Mazzotti M, Vass WC, Beguinot L (1995) SHC and GRB-2 are constitutively activated by an epidermal growth factor receptor with a point mutation in the transmembrane domain. J Biol Chem 270: 19557–19562

Nilges M, Brünger AT (1991) Automated modeling of coiled coils: application to the GCN4 dimerization region. Protein Eng 4: 649–659

O'Shea EK, Klemm JD, Kim PS, Alber T (1991) X-ray structure of the GCN4 leucine zipper, two-stranded, parallel coiled coil. Science 254: 539–544

Popot JL, Engelman DM (1990) Membrane protein folding and oligomerization: the two-stage model. Biochemistry 29: 4031–4037

Rousseau F, Bonaventure J, Legeai-Mallet L, Pelet A, Rozet JM, Maroteaux P, Le Merrer, Munnich A (1994) Mutations in the gene encoding fibroblast growth factor receptor-3 in achondroplasia. Nature 371: 252–254

Sajot N, Garnier N, Genest M (1999) Dimer models for ErbB-2/neu transmembrane domains from molecular dynamics simulations. Theor Chem Acc 101: 67–72

Sankararamakrishnan R, Sansom MSP (1995a) Modelling packing interactions in parallel helix bundles: pentameric bundles of nicotinic receptor M2 helices. Biochim Biophys Acta 1239: 122–132

Sankaramakrishnan R, Sansom MSP (1995b) Structural features of isolated M2 helices of nicotinic receptors. Simulated annealing via molecular dynamics studies. Biophys Chem 55: 215–230

Segatto O, King CR, Pierce JH, Di Fiore PP, Aaronson SA (1988) Different structural alterations upregulate in vivo tyrosine kinase activity and transforming potency of erbB-2 gene. Mol Cell Biol 8: 5570–5574

Shiang R, Thompson LM, Zhu YZ, Church DM, Fielder TJ, Bocian M, Winokur ST, Wasmuth JJ (1994) Mutations in the transmembrane domain of FGFR3 cause the most common genetic form of dwarfism, achondroplasia. Cell 78: 335–342

Smith SO, Smith CS, Bormann BJ (1996) Strong hydrogen bonding interactions involving a buried glutamic acid in the transmembrane sequence of the neu/erbB-2 receptor. Nat Struct Biol 3: 252–258

Stern DF, Kamps MP, Cao H (1988) Oncogenic activation of p185neu stimulates tyrosine phosphorylation in vivo. Mol Cell Biol 8: 3969–3973

Sternberg MJ, Gullick WJ (1989) Neu receptor dimerization. Nature 339: 587

Sternberg MJ, Gullick WJ (1990) A sequence motif in the transmembrane region of growth factor receptors with tyrosine kinase activity mediates dimerization. Protein Eng 3: 245–248

Tieleman DP, Sansom MSP, Berendsen HJC (1999) Alamethicin helices in a bilayer and in solution: molecular dynamics simulations. Biophys J 76: 40–49

Treutlein HR, Lemmon MA, Engelman DM, Brunger AT (1992) The glycophorin A transmembrane domain dimer: sequence-specific propensity for a right-handed supercoil of helices. Biochemistry 31: 12726–12733

Tripos Associates SYBYL, molecular modeling software. Tripos, St Louis, Mo.

Tsukihara T, Aoyama H, Yamashita E, Tomizaki T, Yamaguchi H, Shinzawa-Itoh K, Nakashima R, Yaono R, Yoshikawa S (1996) The whole structure of the 13-subunit oxidized cytochrome c oxidase at 2.8 A. Science 272: 1136–1144

Ullrich A, Schlessinger J (1990) Signal transduction by receptors with tyrosine kinase activity. Cell 61: 203–212

Webster MK, Donoghue DJ (1996) Constitutive activation of fibroblast growth factor receptor 3 by the transmembrane domain point mutation found in achondroplasia. EMBO J 15: 520–527

Weiner DB, Kokai Y, Wada T, Cohen JA, Williams WV, Greene MI (1989a) Linkage of tyrosine kinase activity with transforming ability of the p185neu oncoprotein. Oncogene 4: 1175–1183

Weiner DB, Liu J, Cohen JA, Williams WV, Greene MI (1989b) A point mutation in the neu oncogene mimics ligand induction of receptor aggregation. Nature 339: 230–231

Xia D, Yu CA, Kim H, Xia JZ, Kachurin AM, Zhang L, Yu L, Deisenhofer J (1997) Crystal structure of the cytochrome bc 1 complex from bovine heart mitochondria. Science 277: 60–66

Yamamoto T, Ikawa S, Akiyama T, Semba K, Nomura N, Miyajima N, Saito T, Toyoshima K (1986) Similarity of protein encoded by the human c-erb-B-2 gene to epidermal growth factor receptor. Nature 319: 230–234

Yarden Y, Schlessinger J (1987) Self-phosphorylation of epidermal growth factor receptor: evidence for a model of intermolecular allosteric activation. Biochemistry 26: 1434–1442